U.S. Department of Transportation
Federal Highway Administration

Errata

Date:	April 17, 2019
Issuing Office:	Federal Highway Administration—Office of Research, Development, and Technology
Address:	Turner-Fairbank Highway Research Center, 6300 Georgetown Pike, McLean, VA 22101
Name of Document:	Analysis Procedures for Evaluating Superheavy Load Movement on Flexible Pavements, Volume IV: Appendix C, Material Characterization for Superheavy Load Movement Analysis
FHWA Publication No.:	FHWA-HRT-18-052

The following changes were made to the document after publication on the Federal Highway Administration website:

Location	Incorrect Values	Corrected Values
TECHNICAL REPORT DOCUMENTATION PAGE, Box 15	Nadarajah Sivaneswaran (HRDI-20; ORCID: 0000-0002-3525-9165), Office of Infrastructure Research and Development, Turner-Fairbank Highway Research Center, served as the Contracting Officer's Representative.	Nadarajah Sivaneswaran (HRDI-20; ORCID: 0000-0003-0287-664X), Office of Infrastructure Research and Development, Turner-Fairbank Highway Research Center, served as the Contracting Officer's Representative.

Analysis Procedures for Evaluating Superheavy Load Movement on Flexible Pavements, Volume IV: Appendix C, Material Characterization for Superheavy Load Movement Analysis

*P*UBLICATION NO. FHWA-HRT-18-052

OCTOBER 2018

U.S. Department of Transportation
Federal Highway Administration

Research, Development, and Technology
Turner-Fairbank Highway Research Center
6300 Georgetown Pike
McLean, VA 22101-2296

FOREWORD

The movement of superheavy loads (SHLs) on the Nation's highways is an increasingly common, vital economic necessity for many important industries, such as chemical, oil, electrical, and defense. Many superheavy components are extremely large and heavy (gross vehicle weights in excess of a few million pounds), and they often require specialized trailers and hauling units. At times, SHL vehicles have been assembled to suit the load being transported, and therefore, the axle configurations have not been standard or consistent. Accommodating SHL movements without undue damage to highway infrastructure requires the determination of whether the pavement is structurally adequate to sustain the SHL movement and protect any underground utilities. Such determination involves analyzing the likelihood of instantaneous or rapid load-induced shear failure of the pavement structure.

The goal of this project was to develop a comprehensive analysis process for evaluating SHL movement on flexible pavements. As part of this project, a comprehensive mechanistic-based analysis approach consisting of several analysis procedures was developed for flexible pavement structures and documented in a 10-volume series of Federal Highway Administration reports—a final report and 9 appendices.[1–9] This is *Analysis Procedures for Evaluating Superheavy Load Movement on Flexible Pavements, Volume IV: Appendix C, Material Characterization for Superheavy Load Movement Analysis*, which describes the material characterization required to predict pavement responses within the structure when subjected to an SHL-vehicle movement. This report is intended for use by highway agency pavement engineers responsible for assessing the structural adequacy of pavements in the proposed route and identifying mitigation strategies, where warranted, in support of the agency's response to SHL-movement permit requests.

Cheryl Allen Richter, Ph.D., P.E.
Director, Office of Infrastructure
Research and Development

TECHNICAL REPORT DOCUMENTATION PAGE

1. Report No. FHWA-HRT-18-052	2. Government Accession No.	3. Recipient's Catalog No.
4. Title and Subtitle Analysis Procedures for Evaluating Superheavy Load Movement on Flexible Pavements, Volume IV: Appendix C, Material Characterization for Superheavy Load Movement Analysis		5. Report Date October 2018 6. Performing Organization Code
7. Author(s) Hadi Nabizadeh (ORCID: 0000-0001-8215-1299), Elie Y. Hajj (ORCID: 0000-0001-8568-6360), Raj V. Siddharthan (ORCID: 0000-0002-3847-7934), and Sherif Elfass (ORCID: 0000-0003-3401-6513)		8. Performing Organization Report No. WRSC-UNR-201710-01C
9. Performing Organization Name and Address Department of Civil and Environmental Engineering University of Nevada Reno, NV 89557		10. Work Unit No. 11. Contract or Grant No. DTFH61-13-C-00014
12. Sponsoring Agency Name and Address Office of Infrastructure Research and Development Federal Highway Administration 6300 Georgetown Pike McLean, VA 22101		13. Type of Report and Period Covered Final Report; August 2013–July 2018 14. Sponsoring Agency Code HRDI-20
15. Supplementary Notes Nadarajah Sivaneswaran (HRDI-20; ORCID: 0000-0003-0287-664X*), Office of Infrastructure Research and Development, Turner-Fairbank Highway Research Center, served as the Contracting Officer's Representative.		
16. Abstract The movement of superheavy loads (SHLs) has become more common over the years, since it is a vital necessity for many important industries, such as chemical, oil, electrical, and defense. SHL hauling units are much larger in size and weight compared to standard trucks. SHL vehicles' gross vehicle weights may be in excess of a few million pounds, so they often require specialized trailers and components with nonstandard spacing between the tires and axles. Accommodating SHL movement requires the determination of whether the pavement is structurally adequate and involves the analysis of the likelihood of instantaneous or rapid load-induced shear failure. As part of this Federal Highway Administration project, Analysis Procedures for Evaluating Superheavy Load Movement on Flexible Pavements, procedures for characterizing properties of the existing pavement layers were developed. This report describes the material characterization required to predict pavement responses (stresses, strains, and deflections) within the pavement structure when subjected to SHL-vehicle movement. An overall step-by-step procedure is presented for determining the damaged dynamic modulus master curve for the asphalt-concrete layer. An analogous procedure is also presented for determining the resilient modulus of unbound materials as a function of the state of stresses based on falling weight deflectometer measurements.		
17. Key Words Superheavy load, flexible pavement, damaged dynamic modulus, resilient modulus, nondestructive testing	18. Distribution Statement No restrictions. This document is available to the public through the National Technical Information Service, Springfield, VA 22161. http://www.ntis.gov	

19. Security Classif. (of this report) Unclassified	20. Security Classif. (of this page) Unclassified	21. No. of Pages 34	22. Price N/A

Form DOT F 1700.7 (8-72) Reproduction of completed page authorized.

*Revised 4/17/19

SI* (MODERN METRIC) CONVERSION FACTORS

APPROXIMATE CONVERSIONS TO SI UNITS

Symbol	When You Know	Multiply By	To Find	Symbol
		LENGTH		
in	inches	25.4	millimeters	mm
ft	feet	0.305	meters	m
yd	yards	0.914	meters	m
mi	miles	1.61	kilometers	km
		AREA		
in^2	square inches	645.2	square millimeters	mm^2
ft^2	square feet	0.093	square meters	m^2
yd^2	square yard	0.836	square meters	m^2
ac	acres	0.405	hectares	ha
mi^2	square miles	2.59	square kilometers	km^2
		VOLUME		
fl oz	fluid ounces	29.57	milliliters	mL
gal	gallons	3.785	liters	L
ft^3	cubic feet	0.028	cubic meters	m^3
yd^3	cubic yards	0.765	cubic meters	m^3
		NOTE: volumes greater than 1000 L shall be shown in m^3		
		MASS		
oz	ounces	28.35	grams	g
lb	pounds	0.454	kilograms	kg
T	short tons (2000 lb)	0.907	megagrams (or "metric ton")	Mg (or "t")
		TEMPERATURE (exact degrees)		
^oF	Fahrenheit	5 (F-32)/9 or (F-32)/1.8	Celsius	^oC
		ILLUMINATION		
fc	foot-candles	10.76	lux	lx
fl	foot-Lamberts	3.426	$candela/m^2$	cd/m^2
		FORCE and PRESSURE or STRESS		
lbf	poundforce	4.45	newtons	N
lbf/in^2	poundforce per square inch	6.89	kilopascals	kPa

APPROXIMATE CONVERSIONS FROM SI UNITS

Symbol	When You Know	Multiply By	To Find	Symbol
		LENGTH		
mm	millimeters	0.039	inches	in
m	meters	3.28	feet	ft
m	meters	1.09	yards	yd
km	kilometers	0.621	miles	mi
		AREA		
mm^2	square millimeters	0.0016	square inches	in^2
m^2	square meters	10.764	square feet	ft^2
m^2	square meters	1.195	square yards	yd^2
ha	hectares	2.47	acres	ac
km^2	square kilometers	0.386	square miles	mi^2
		VOLUME		
mL	milliliters	0.034	fluid ounces	fl oz
L	liters	0.264	gallons	gal
m^3	cubic meters	35.314	cubic feet	ft^3
m^3	cubic meters	1.307	cubic yards	yd^3
		MASS		
g	grams	0.035	ounces	oz
kg	kilograms	2.202	pounds	lb
Mg (or "t")	megagrams (or "metric ton")	1.103	short tons (2000 lb)	T
		TEMPERATURE (exact degrees)		
^oC	Celsius	1.8C+32	Fahrenheit	^oF
		ILLUMINATION		
lx	lux	0.0929	foot-candles	fc
cd/m^2	$candela/m^2$	0.2919	foot-Lamberts	fl
		FORCE and PRESSURE or STRESS		
N	newtons	0.225	poundforce	lbf
kPa	kilopascals	0.145	poundforce per square inch	lbf/in^2

ANALYSIS PROCEDURES FOR EVALUATING SUPERHEAVY LOAD MOVEMENT ON FLEXIBLE PAVEMENTS PROJECT REPORT SERIES

This volume is the fourth of 10 volumes in this research report series. Volume I is the final report, and Volume II through Volume X consist of Appendix A through Appendix I. Any reference to a volume in this series will be referenced in the text as "Volume II: Appendix A," "Volume III: Appendix B," and so forth. The following list contains the volumes:

Volume	Title	Report Number
I	Analysis Procedures for Evaluating Superheavy Load Movement on Flexible Pavements, Volume I: Final Report	FHWA-HRT-18-049
II	Analysis Procedures for Evaluating Superheavy Load Movement on Flexible Pavements, Volume II: Appendix A, Experimental Program	FHWA-HRT-18-050
III	Analysis Procedures for Evaluating Superheavy Load Movement on Flexible Pavements, Volume III: Appendix B, Superheavy Load Configurations and Nucleus of Analysis Vehicle	FHWA-HRT-18-051
IV	Analysis Procedures for Evaluating Superheavy Load Movement on Flexible Pavements, Volume IV: Appendix C, Material Characterization for Superheavy Load Movement Analysis	FHWA-HRT-18-052
V	Analysis Procedures for Evaluating Superheavy Load Movement on Flexible Pavements, Volume V: Appendix D, Estimation of Subgrade Shear Strength Parameters Using Falling Weight Deflectometer	FHWA-HRT-18-053
VI	Analysis Procedures for Evaluating Superheavy Load Movement on Flexible Pavements, Volume VI: Appendix E, Ultimate and Service Limit Analyses	FHWA-HRT-18-054
VII	Analysis Procedures for Evaluating Superheavy Load Movement on Flexible Pavements, Volume VII: Appendix F, Failure Analysis of Sloped Pavement Shoulders	FHWA-HRT-18-055
VIII	Analysis Procedures for Evaluating Superheavy Load Movement on Flexible Pavements, Volume VIII: Appendix G, Risk Analysis of Buried Utilities Under Superheavy Load Vehicle Movements	FHWA-HRT-18-056
IX	Analysis Procedures for Evaluating Superheavy Load Movement on Flexible Pavements, Volume IX: Appendix H, Analysis of Cost Allocation Associated with Pavement Damage Under a Superheavy Load Vehicle Movement	FHWA-HRT-18-057
X	Analysis Procedures for Evaluating Superheavy Load Movement on Flexible Pavements, Volume X: Appendix I, Analysis Package for Superheavy Load Vehicle Movement on Flexible Pavement (SuperPACK)	FHWA-HRT-18-058

TABLE OF CONTENTS

LIST OF FIGURES

LIST OF TABLES

LIST OF ABBREVIATIONS AND SYMBOLS

Abbreviations

AASHTO	American Association of State Highway and Transportation Officials
AC	asphalt concrete
CAB	crushed aggregate base
FWD	falling weight deflectometer
ME	mechanistic–empirical
No.	number
PG	performance grade
SG	subgrade
SHA	state highway agency
SHL	superheavy load

Symbols

A	intercept of viscosity–temperature susceptibility relationship
$a(T)$	shift factor as a function of temperature
$c_{f\text{-}bot}$	field-calibrated fitting parameters for alligator cracking
c_{shift}	fitting parameter of dynamic modulus shifting factor
d_{AC}	fatigue damage in AC layer
$d_{f\text{-}bot}$	field-calibrated fitting parameters for damage in alligator cracking
e	exponential function
E^*	dynamic modulus
E^*_{dam}	existing AC-layer modulus
E_{FWD}	falling weight deflectometer backcalculated modulus
E_{PRED}	predicted modulus
E^*_{undam}	undamaged AC-layer modulus
f	loading frequency
FC_{AC}	area of alligator cracking as a percent of total lane area
G^*	shear modulus
H_{AC}	thickness of AC layer
K	regression constant of resilient modulus model
m	deviator stress exponent
M_R	resilient modulus
n	bulk stress exponent
t	time of loading at the temperature of interest
t_{FWD}	falling weight deflectometer reduced time
t_r	time of loading at the reference temperature
T_R	temperature on Rankine scale
V_a	air void
V_{beff}	effective binder content
VTS	slope of viscosity–temperature susceptibility relationship
α	fitting parameter describing the difference between maximum and minimum of the E^* master curve

α'	fitting parameter describing the difference between maximum and minimum of the damaged E^* master curve
β	fitting parameter describing the shape of the sigmoid function
γ	fitting parameter for t_r in describing the shape of the sigmoid function
δ	fitting parameter describing the minimum of the E^* master curve
δ_b	phase angle
ε_r	recoverable strain
η	viscosity
η_{ref}	viscosity at reference temperature
θ	bulk stress
$\rho_{3/4}$	cumulative percent retained on 3/4-inch sieve
$\rho_{3/8}$	cumulative percent retained on 3/8-inch sieve
ρ_4	cumulative percent retained on No. 4 sieve
ρ_{200}	percent passing No. 200 sieve
σ_1	major principal stress
σ_2	intermediate principal stress
σ_3	minor principal stress
σ_c	confining stress
σ_d	deviator stress
σ_{ij}	stress tensor
σ_{oct}	octahedral normal stress
τ_{oct}	octahedral shear stress

CHAPTER 1. INTRODUCTION

Pavement responses are critical inputs to assess the risk of instantaneous shear failure in the pavement structure under superheavy load (SHL)-vehicle movement. In addition, investigating sloped-shoulder failure, risk analysis of buried utilities, service limit failure criteria, and pavement damage–associated costs requires reliable estimations of pavement responses during SHL-vehicle movements. Therefore, one of the major tasks in this project was to estimate pavement responses (i.e., stress, strain, and deflections) under SHL-vehicle movements. In general, focus is given to understanding the role of governing factors, such as lower SHL-vehicle speeds compared to those of normal trucks, pavement-layer material properties that are consistent with SHL loading, and nonstandard vehicle loading (e.g., tire configuration, tire loading, and inflation pressure).

A critical input when analyzing SHL-vehicle movements using numerical models is the material properties of the existing pavement layers. These properties should appropriately represent the characteristics of the materials that exist at the time of the SHL movement. Dynamic modulus (E^*) is the primary material property of asphalt-concrete (AC) layers and is a function of temperature and loading frequency. The stiffness of unbound layers, such as the crushed aggregate base (CAB) and the subgrade (SG), is affected by load-induced stresses independent of loading frequency.

Nonetheless, it is routine to assume pavement layers are linear elastic when considering customary truck-traffic loading. This assumption may result in an inappropriate estimation of pavement responses under slow-moving SHL vehicles, which often have nonconventional axle configurations and tire loadings. The following two main concerns need to be addressed when analyzing SHL movements:

- SHL vehicles usually move at a lower operational speed (typically at 10 to 30 mph) than standard traffic. Hence, the role of lower speed needs to be addressed when characterizing the existing AC layer.

- Since the resilient modulus (M_R) of unbound layers is stress-dependent, it is essential to consider the effect of the load-induced state of stresses in the stiffness properties (i.e., M_R) of unbound layers.

1.1. OBJECTIVES AND SCOPE OF WORK

As part of this Federal Highway Administration project, Analysis Procedures for Evaluating Superheavy Load Movement on Flexible Pavements, a comprehensive mechanistic-based analysis approach consisting of several analysis procedures was developed. A summary of the various analysis procedures developed and the associated objectives (including related volume numbers) are summarized in table 1. This report (Volume IV: Appendix C) is the fourth of 10 volumes and presents the procedures for characterizing existing pavement materials for SHL-movement analysis.

Table 1. Developed analysis procedures to evaluate SHL movement on flexible pavements.

Procedure	Objective
SHL analysis vehicle	Identify segment(s) of the SHL vehicle configuration that can be regarded as representative of the entire SHL vehicle (Volume III: Appendix B)[3]
Flexible pavement structure	Characterize representative material properties for existing pavement layers (Volume IV: Appendix C and Volume V: Appendix D)[4]
SG bearing failure analysis	Investigate instantaneous ultimate shear failure in pavement SG (Volume VI: Appendix E)[5]
Sloped-shoulder failure analysis	Examine the stability of sloped pavement shoulders under SHL-vehicle movement (Volume VII: Appendix F)[6]
Buried utility risk analysis	Perform risk analysis of existing buried utilities (Volume VIII: Appendix G)[7]
Localized shear failure analysis	Inspect the likelihood of localized failure (yield) in the pavement SG (Volume VI: Appendix E)[2]
Deflection-based service limit analysis	Investigate the development of premature surface distresses (Volume VI: Appendix E)[5]
Cost allocation analysis	Determine pavement damage–associated cost attributable to SHL-vehicle movement (Volume IX: Appendix H)[8]

The 3D-Move Analysis software is an efficient, dynamic finite layer–based model that uses a frequency domain approach to calculate pavement responses under static and dynamic (i.e., moving) surface loads.[10] The software can account for the viscoelastic properties of the AC layer and the nonuniform tire–pavement interface stresses (normal and shear) on any shape-loaded area. As detailed in chapter 2, the use of the E^* master curve for the AC layer, which is a readily accepted input for the 3D-Move Analysis software approach, can address the issue related to the lower SHL-vehicle speed (i.e., the role of the SHL-vehicle speed). Furthermore, with the use of the master curve, it is possible to account for the difference in temperature between the time of the falling weight deflectometer (FWD) measurement and the time of the SHL-vehicle movement. Under such circumstances, the 3D-Move Analysis software was seen as an ideal candidate to evaluate pavement responses. In this report, the approach to developing an E^* master curve for an existing AC layer to use with the 3D-Move Analysis software is presented.

Though the finite element method may be used to characterize the nonlinear stress-dependent behavior of unbound materials, a much simpler FWD-based approach has been adopted. In this approach, the finite layer–based 3D-Move Analysis software, which uses a uniform layer stiffness value that does not vary in lateral direction, is used in conjunction with appropriately selected uniform stiffness values for the existing unbound pavement layers. This approach is described in this report.

CHAPTER 2. CHARACTERIZATION OF ASPHALT CONCRETE MATERIALS

*E** is the most important asphalt-mixture material property that is used in mechanistic–empirical (ME) pavement analysis and design procedures, such as the *Mechanistic–Empirical Pavement Design Guide*.[11] *E** measurement considers the frequency and temperature dependency of an asphalt material.

Samples of asphalt mixtures are usually subjected to sinusoidal cyclic axial loading with varying frequencies at different temperatures (i.e., a *E** test). The amplitude of *E** is strongly dependent on the testing temperature and frequency of the loading. By conducting a series of *E** tests at various temperatures and frequencies, the *E** master curve can be developed. The master curve is a representation of *E** as a function of temperature and *f*. Figure 1 shows the *E** master curve for an asphalt mixture at two different temperatures. *E** increases with an increase in *f* or a decrease in temperature. The *E** versus *f* relationship at the appropriate AC-layer temperature can be derived from a master curve.

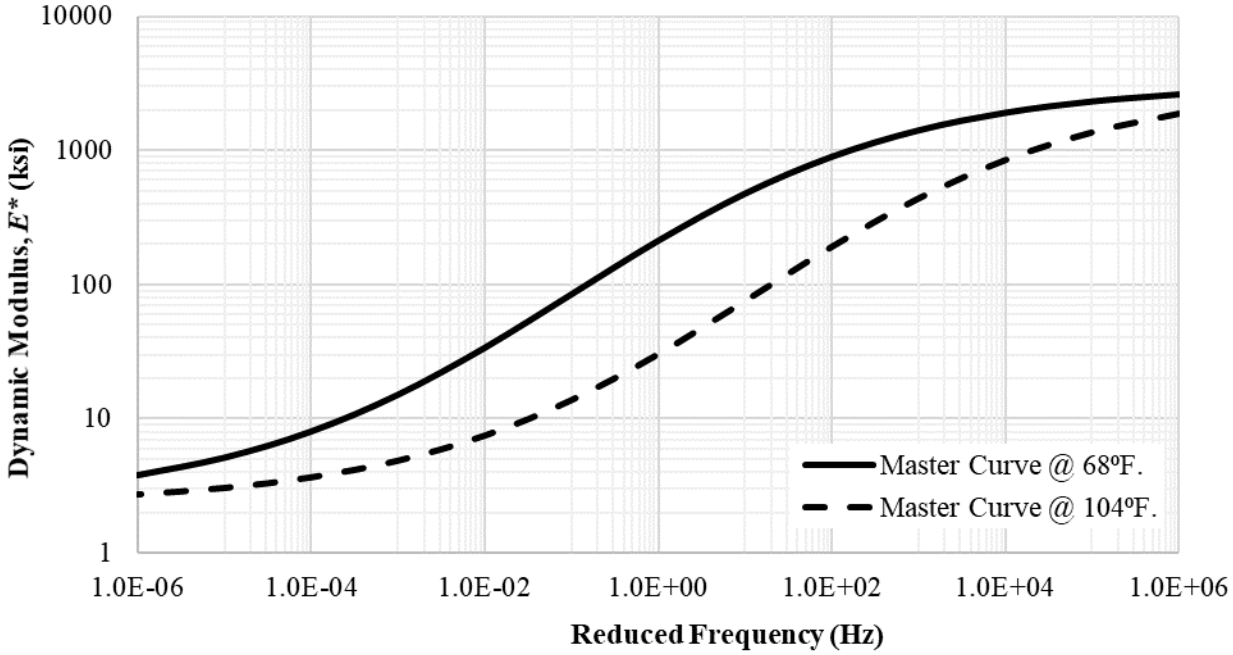

Figure 1. Graph. Typical *E master curve for an asphalt mixture.**

2.1. OVERVIEW OF *E** MASTER CURVE DEVELOPMENT

A master curve is constructed using the principle of time–temperature superposition by shifting the measured *E** data at different temperatures to a reference temperature with respect to *f*. This process continues until the data merge into a single, smooth curve (figure 2). As depicted in figure 3, the temperature dependency of the material is represented by the amount of shifting required at each temperature to form the master curve. The shift factor is a direct function of temperature ($a(T)$).

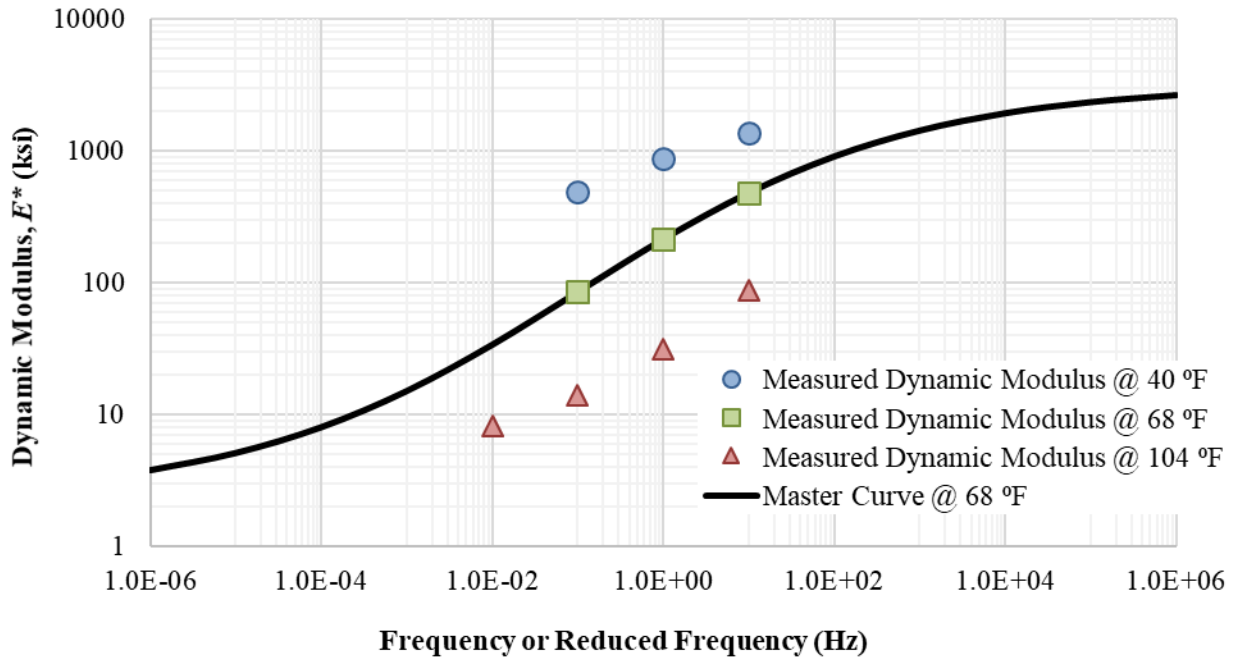

Figure 2. Graph. Construction of *E master curve.**

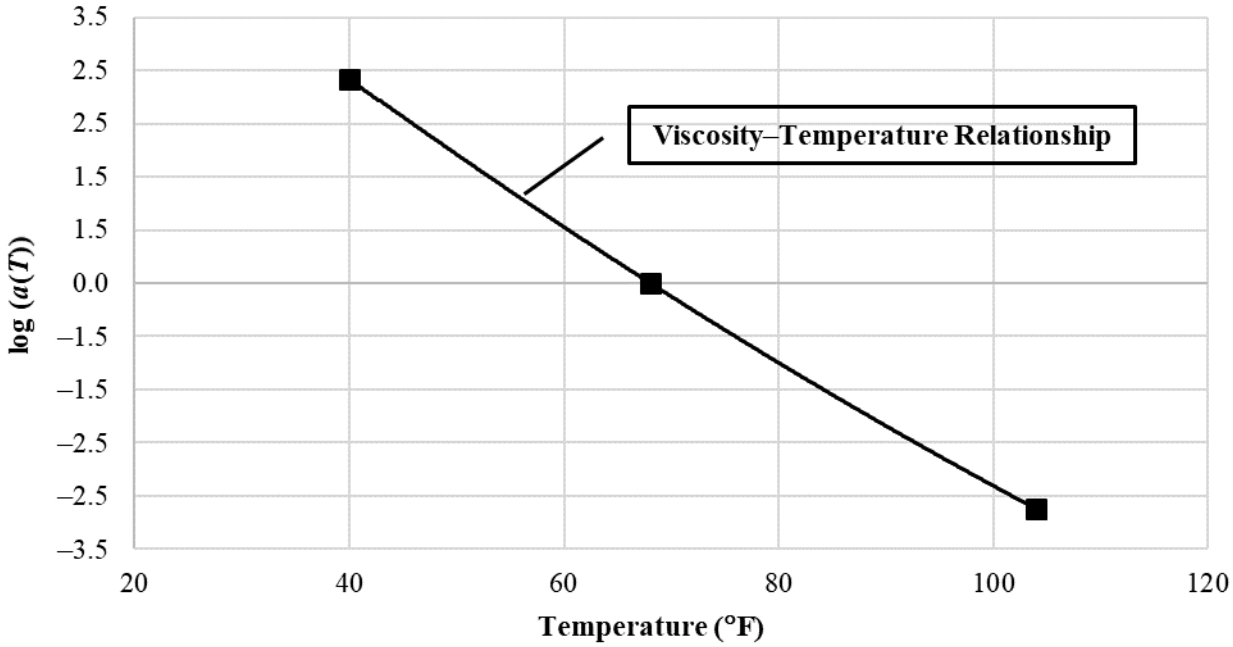

Figure 3. Graph. *a*(*T*).

The *E** master curve is represented by a sigmoid function expressed by the equation in figure 4. The *a*(*T*) is described by the equation in figure 5. Since the viscosity (η) of an asphalt binder is a function of temperature, the shift factor can be determined as a function of η (figure 6).[(11)]

$$log(E^*) = \delta + \frac{\alpha}{1 + e^{\beta + \gamma log(t_r)}}$$

Figure 4. Equation. Sigmoid function for *E master curve.**

$$log(a(T)) = log(t) - log(t_r)$$

Figure 5. Equation. *a*(*T*).

$$log(a(T)) = c_{shift}(\log(\eta) - \log(\eta_{ref}))$$

Figure 6. Equation. Shift factor as a function of η.

Where:

e = exponential function.
t_r = time of loading at the reference temperature.
α = fitting parameter describing the difference between maximum and minimum of the E^* master curve.
δ = fitting parameter describing the minimum of the E^* master curve.
β = fitting parameter describing the shape of the sigmoid function.
γ = fitting parameter for t_r in describing the shape of the sigmoid function.
t = time of loading at the temperature of interest.
η_{ref} = η at reference temperature.
c_{shift} = fitting parameter of E^* shifting factor.

The equations given in figure 4 through figure 6 can be combined to arrive at the master curve sigmoid function expressed by the equation in figure 7. It should be noted that α, δ, β, γ, and c_{shift} are determined by nonlinear optimization.

$$log(E^*) = \delta + \frac{\alpha}{1 + e^{\beta + \gamma\left[log(t) - c_{shift}\left(log(\eta) - log(\eta_{ref})\right)\right]}}$$

Figure 7. Equation. Sigmoid function for *E master curve as a function of asphalt-binder η.**

The relationship between asphalt-binder η and temperature is highly nonlinear. However, when η and temperature are properly transformed, a linear relationship exists between these parameters.(12) The viscosity–temperature susceptibility relationship, which is commonly referred to as the *A*-*VTS* relationship, is shown in figure 8.

$$log(log(\eta)) = A + VTS \cdot log(T_R)$$

Figure 8. Equation. Viscosity–temperature susceptibility relationship.

Where:

T_R = temperature on Rankine scale.
A = intercept of the viscosity–temperature susceptibility relationship.
VTS = slope of the viscosity–temperature susceptibility relationship.

Accordingly, by knowing *A* and *VTS* parameters, η of the asphalt binder at the temperature of interest can be determined.

2.2. FIELD-DAMAGED *E** MASTER CURVE

It is obvious that a deteriorated pavement is more vulnerable to failure and further deterioration under traffic loading, particularly when it is subjected to nonconventional SHL-vehicle movement. Therefore, the pavement material properties used in the pavement analysis under an SHL movement should represent the actual condition of a pavement structure. For the AC layer, reduction in the AC-layer stiffness because of existing damage (i.e., cracking) can be addressed by using the field-damaged *E** master curve.

This section presents a step-by-step approach to establishing the *E** master curve for an existing AC layer, which is referred to as the field-damaged *E** master curve. Figure 9 illustrates the overall approach, which is expanded from the current approach used in the American Association of State Highway and Transportation Officials' (AASHTO's) AASHTOWare® Pavement ME software when conducting a rehabiliation design of AC overlay of AC pavements.[11,13]

The approach consists of determining the field-damaged *E** master curve of the existing AC layer by following two major steps: the determination of the viscosity–temperature susceptibility relationship of the asphalt binder (step 1) and the construction of the damaged *E** master curve (step 2). Step 1 is accomplished by either calculating *A* and *VTS* parameters from measured data (option 1A) or by estimating *A* and *VTS* parameters from a database. The second step is accomplished by either collecting and conducting *E** testing on cores from the wheel path (option 2A) or by estimating the damaged *E** master curve (option 2B). The latter first requires the characterization of the undamaged *E** master curve, which can be done by either collecting and conducting *E** testing on cores from between the wheel paths (option 2B-1A) or by using the Witczak predictive model.[11] The predictive model requires inputs related to asphalt-binder properties, aggregate gradation, and mixture volumetric properties that can be determined from testing on core samples collected from between the wheel paths or estimated from historical data. The final step under option 2B is to characterize the damage due to fatigue cracking in the AC layer. This is done by either conducting FWD testing in the most trafficked wheel path (option 2B-2A) or by estimating the damage from a condition survey (option 2B-2B) or a general condition rating (option 2B-2C).

In this step-by-step approach, the damaged *E** of the AC layer can be determined either from laboratory testing of core samples collected directly from the pavement where the SHL movement is anticipated to take place or from nondestructive techniques through the use of FWD measurements along with field survey data and historical data. Figure 10 shows the measurements and properties needed for determining the damaged *E** of the AC layer from testing core samples or from nondestructive techniques. The following sections describe in detail the various steps of the approach.

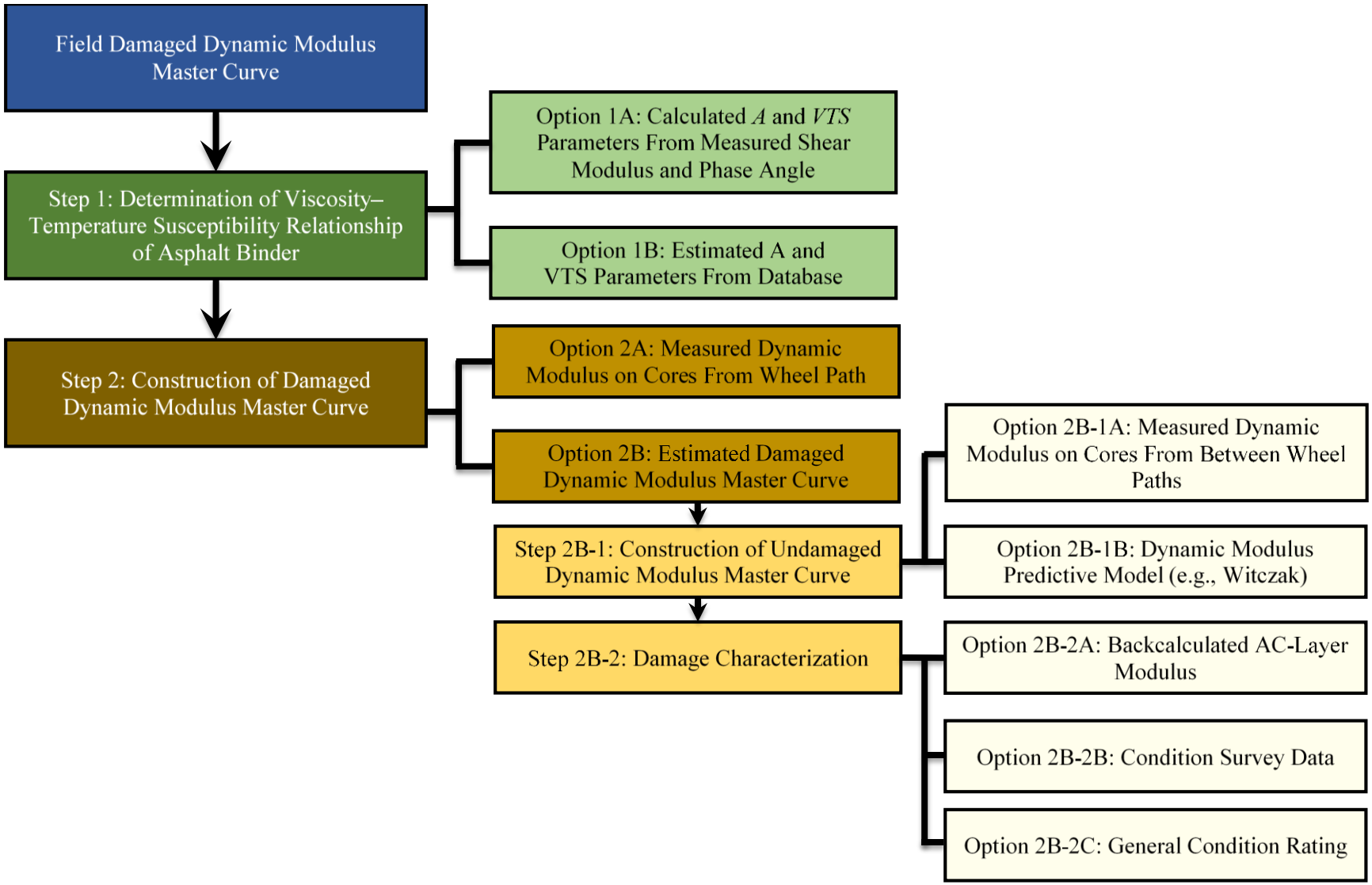

Figure 9. Flowchart. Step-by-step approach for determining the field-damaged *E master curve of the AC layer.**

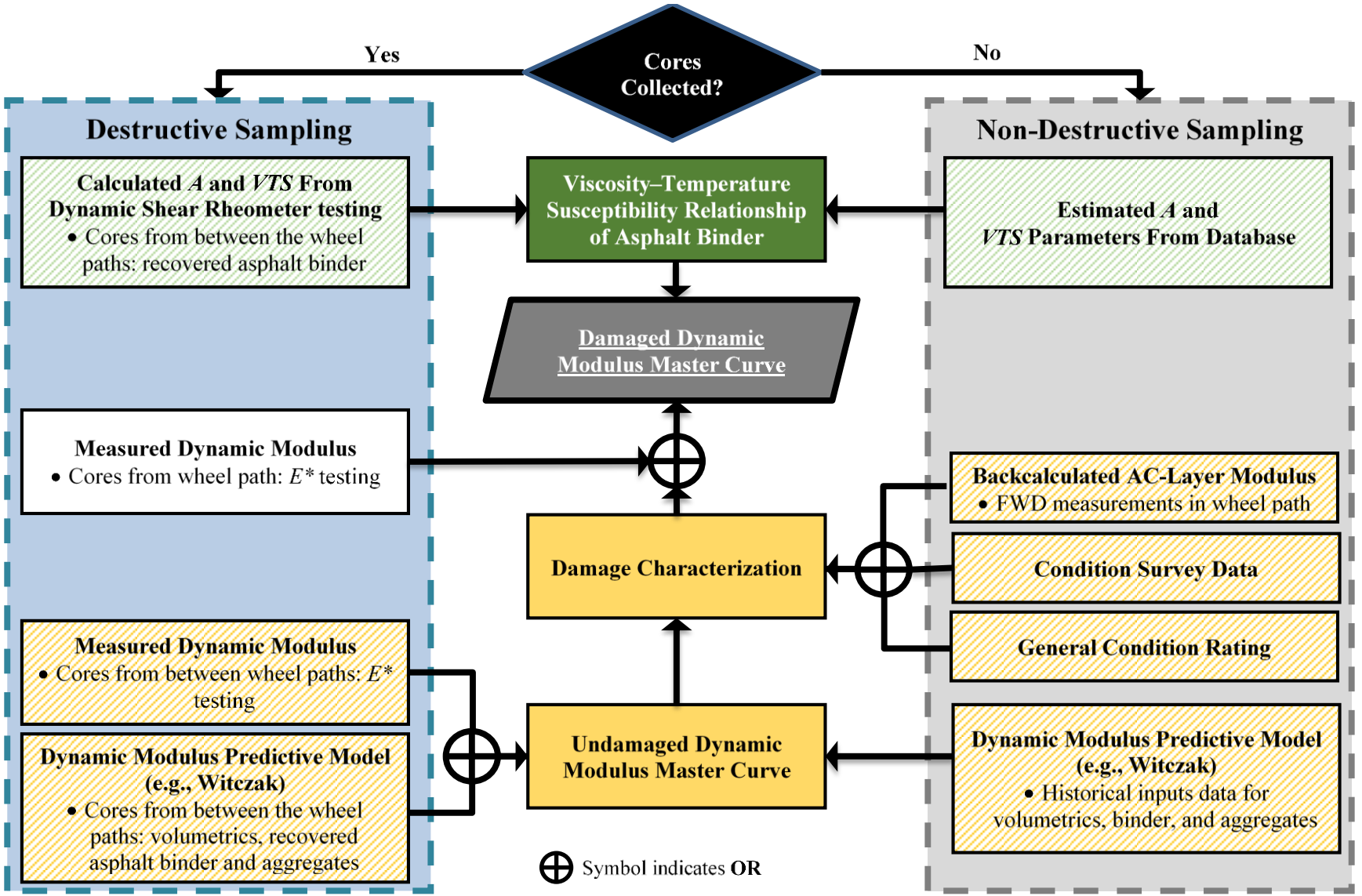

Figure 10. Flowchart. Estimation of the damaged *E for AC layer.**

2.2.1. Determination of Viscosity–Temperature Susceptibility (Step 1)

As shown in figure 9, the first step to establish the damaged *E** master curve for the existing AC layer is to determine the viscosity–temperature susceptibility relationship for the asphalt binder used in the asphalt mixture. Two options were considered for determining *A* and *VTS* parameters: calculating directly from measured rheological properties of the asphalt binder (option 1A) or estimating from a database of *A*–*VTS* values based on asphalt-binder grade (option 1B). These options are described in the following sections.

Option 1A: Calculated A *and* VTS *Parameters From Measured Shear Modulus and Phase Angle*

The asphalt binder's shear modulus (*G**) and phase angle (δ_b) obtained from dynamic shear rheometer testing (AASHTO T 315) at certain temperatures (at least three temperatures) are used in the equation in figure 11 to calculate η of the asphalt binder at the respective temperatures.[11,14] Using the calculated η and the equation in figure 8, *A* and *VTS* parameters are calculated. It should be noted that a representative asphalt binder recovered from the existing AC layer should be used in this process. The AASHTO T 319 procedure can be used to extract and recover the asphalt binder from core samples collected from between the wheel paths (referred to as undamaged core samples).[15]

$$\eta = \frac{G^*}{10}\left(\frac{1}{sin(\delta_b)}\right)^{4.8628} \times 1000$$

Figure 11. Equation. Asphalt-binder viscosity as a function of *G and phase angle.**

Note that η is in centipoises, *G** is in pascals, and δ_b is in degrees.

Option 1B: Estimated A *and* VTS *Parameters From Database*

The viscosity–temperature susceptibility (*A* and *VTS*) parameters can be estimated using the performance grade (PG), viscosity grade, or penetration grade of asphalt binders. Table 2 through table 4 represent the recommended *A* and *VTS* parameters based on asphalt binders' PG, penetration grade, and viscosity grade, respectively.[11]

Table 2. Recommended *A* and *VTS* parameters based on asphalt binders' PG.

LT→	−10	−10	−16	−16	−22	−22	−28	−28	−34	−34	−40	−40	−46	−46
HT ↓	*VTS*	*A*	*VTS*	*A*	*VTS*	*A*	*VTS*	*A*	*VTS*	*A*	*VTS*	*A*	*VTS*	*A*
46	—	—	—	—	—	—	—	—	−3.901	11.504	−3.393	10.101	−2.905	8.755
52	−4.570	13.386	−4.541	13.305	−4.342	12.755	−4.012	11.840	−3.602	10.707	−3.164	9.496	−2.736	8.310
58	−4.172	12.316	−4.147	12.248	−3.981	11.787	−3.701	11.010	−3.350	10.035	−2.968	8.976	—	—
64	−3.842	11.432	−3.822	11.375	−3.680	10.980	−3.440	10.312	−3.134	9.461	−2.798	8.524	—	—
70	−3.566	10.690	−3.548	10.641	−3.426	10.299	−3.217	9.715	−2.948	8.965	−2.648	8.129	—	—
76	−3.331	10.059	−3.315	10.015	−3.208	9.715	−3.024	9.200	−2.785	8.532	—	—	—	—
82	−3.128	9.514	−3.114	9.475	−3.019	9.209	−2.856	8.750	−2.642	8.151	—	—	—	—

LT = low-temperature grade; HT = high-temperature grade.
—No data.

Table 3. Recommended *A* and *VTS* parameters based on asphalt binders' penetration grade.

Penetration Grade	*A*	*VTS*
40–50	10.5254	−3.5047
60–70	10.6508	−3.5537
85–100	11.8232	−3.6210
120–150	11.0897	−3.7252
200–300	11.8107	−4.0068

Table 4. Recommended *A* and *VTS* parameters based on asphalt binders' viscosity grade.

Penetration Grade	*A*	*VTS*
AC-2.5	11.5167	−3.8900
AC-5	11.2614	−3.7914
AC-10	11.0134	−3.6954
AC-20	10.7709	−3.6017
AC-30	10.6316	−3.5480
AC-40	10.5338	−3.5104

2.2.2. Construction of Damaged *E** Master Curve (Step 2)

The role of damage due to fatigue cracking in the AC layer should be reflected in the stiffness property of the asphalt mixture through a field-damaged *E** master curve. After determining the *A* and *VTS* parameters, the field-damaged *E** master curve for the existing AC layer can be developed using one of the following two options, as seen in figure 9: directly measuring the *E** property of an AC field core sampled from the most trafficked wheel path (option 2A) or estimating the *E** from a comparison between the undamaged *E** for the asphalt material between wheel paths and the backcalculated modulus from FWD measurements conducted in the most trafficked wheel path (option 2B). These two options are described in the following sections.

Option 2A: Measured* E* *on Cores From Wheel Path

Pavement deterioration is expected to start and continually accumulate in the wheel path. When conducting *E** tests on the cores obtained from the wheel path, the role of accumulated AC damage (i.e., fatigue cracking) will be reflected in the stiffness property of the AC layer. Therefore, the measured *E** test results at different temperatures and frequencies conducted on wheel-path cores according to AASHTO T 378 should be used to develop the *E** master curve for the existing AC layer.[16]

It should be noted that, according to AASHTO T 378, *E** testing is performed on test specimens that are 4 inches in diameter by 6 inches tall.[16] However, the following two circumstances might be encountered in the field based on the total thickness of the existing AC layer:

- **The total thickness of the AC layer is greater than or equal to 6 inches.** In this case, the *E** test (in accordance with AASHTO T 378) can be performed on a 6-inch-tall specimen cored vertically from the constructed AC layers. However, the existing AC layer will most likely be composed of multiple lifts (typically in 2- to 3-inch lifts) of either the same asphalt-mixture type or asphalt mixtures with different types or ages (e.g., a wearing course AC layer placed on top of a binder course AC layer or an AC overlay placed on top of an existing AC layer). In either case, the *E** test should be conducted on a representative 6-inch core sample assuming that a good bond exists between the different lifts. In the case of a core sample composed of lifts with asphalt mixtures of different types or ages, the measured *E** is considered to be an equivalent modulus for the total AC-layer thickness that can be used to calculate pavement responses under SHL-vehicle movement. This is consistent with the FWD backcalculation standard of practice where these different lifts are combined together, and a single FWD backcalculated modulus (E_{FWD}) is determined for the entire AC layer.

- **The total thickness of the AC layer is less than 6 inches.** In this case, test specimens smaller than the standard geometry (i.e., 4 inches in diameter by 6 inches tall) can be obtained from the existing AC layers to measure *E**. According to AASHTO T 378, the *E** test can be performed on test specimens that are 1.5 inches in diameter by 4.3 inches tall. The specimens can be cored horizontally from within the bounds of construction lifts that are at least 2 inches thick. In this case, for the calculation of pavement responses under SHL-vehicle movement, the lifts can be modeled as two separate sublayers using

their respective measured *E** properties. In the case where the lifts are composed of the same asphalt-mixture type, *E** can be measured on one of the lifts and assumed to be the same for both lifts. It is important to recognize the fact that the stiffness values of the asphalt mixture from the two separate lifts are likely to vary as a result of differences in the in-place density and in the asphalt-binder oxidation level throughout the AC-layer depth.

Option 2B: Estimated Damaged* E* *Master Curve

In order to estimate the field-damaged *E** master curve, the undamaged master curve needs to be determined first (step 2B-1) either by directly measuring *E** on core samples collected from between wheel paths (option 2B-1A) or by estimating the undamaged *E** using a predictive model such as the Witczak predictive equation (option 2B-1B). The two options for establishing an undamaged *E** master curve are represented in figure 9.

In option 2B-1A, *E** testing on specimens cored from between the wheel paths is conducted in accordance with AASHTO T 378.[16] Refer to the discussion in section 2.2.2, Option 2A: Measured Dynamic Modulus on Cores From Wheel Path, for further details. It should be noted that, when a state highway agency (SHA) tests field-core samples, collecting cores from the wheel path is preferred, allowing for a direct measurement of the damaged *E** of the AC layer. However, some SHAs may restrict the sampling of cores from the wheel path and allow it only between the wheel paths. In such circumstances, option 2B-1A would be applicable.

In a case when measured *E** data on cores between the wheel paths are not available, the master curve for the undamaged *E** can be developed from the Witczak predictive equation shown in figure 12 (option 2B-1B).[11] The predictive model incorporates mixture volumetrics, aggregate gradation, and asphalt-binder η of the asphalt mixture under consideration.

$$log(E^*) = -1.249937 + 0.02923\rho_{200} - 0.001767(\rho_{200})^2 - 0.002841\rho_4 - 0.05809V_a - 0.82208\frac{V_{beff}}{V_{beff} + V_a} + \frac{3.871977 - 0.0021\rho_4 + 0.003958(\rho_{3/8}) - 0.000017(\rho_{3/8})^2 + 0.00547\rho_{3/4}}{1 + e^{(-0.603313 - 0.313351\, log(f) - 0.393532\, log(\eta))}}$$

Figure 12. Equation. Predictive *E master curve.**

Where:

ρ_{200} = percent passing number (No.) 200 sieve.
ρ_4 = cumulative percent retained on No. 4 sieve.
V_a = air void (percent by volume).
V_{beff} = effective binder content (percent by volume).
$\rho_{3/8}$ = cumulative percent retained on 3/8-inch sieve.
$\rho_{3/4}$ = cumulative percent retained on 3/4-inch sieve.

The various inputs for the Witczak model can be determined either from testing of core samples collected from between the wheel paths or estimated from historical data. The mixture volumetrics can be determined by testing the core samples in accordance with AASHTO T 166 and AASHTO T 209.[17,18] AASHTO T 319 can be used to extract and recover the asphalt binder and aggregates from the core samples.[15] The recovered asphalt binder can be tested in

accordance with AASHTO T 315 in order to determine the asphalt-binder η.[14] The recovered aggregates can be used for sieve analysis in accordance with AASHTO T 30.[19]

Once the undamaged E^* is determined, the next step is to incorporate the existing AC damage (i.e., cracking) to obtain the damaged E^* master curve of the AC layer. As expressed in figure 13, the role of existing damage in the stiffness properties of the AC layer can be considered by adjusting the E^* computed from the undamaged master curve.[11]

$$E^*_{dam} = 10^{\delta} + \frac{E^*_{undam} - 10^{\delta}}{1 + e^{-0.3 + 5log(d_{AC})}}$$

Figure 13. Equation. Damage-adjusted *E master curve.**

Where:

E^*_{dam} = existing AC-layer modulus.
E^*_{undam} = undamaged AC-layer modulus.
d_{AC} = fatigue damage in AC layer.

d_{AC} can be determined using FWD measurements (option 2B-2A), condition survey data (option 2B-2B), or a general condition rating (option 2B-2C), as shown in figure 9. It should be noted that the FWD analysis is expected to provide a more accurate estimation for the AC damage and subsequent field-damaged E^* master curve.[11]

In option 2B-2A, the estimation of d_{AC} using FWD measurements requires the following inputs: E_{FWD} of the AC layer, FWD *f* or FWD reduced time (t_{FWD}), and temperature at the middepth of the AC layer at the time of FWD testing. The damaged E^* master curve is obtained through a vertical downward shift of E^*_{undam} in such a way that it passes through E_{FWD} at the corresponding FWD *f* and AC-layer temperature (figure 14).

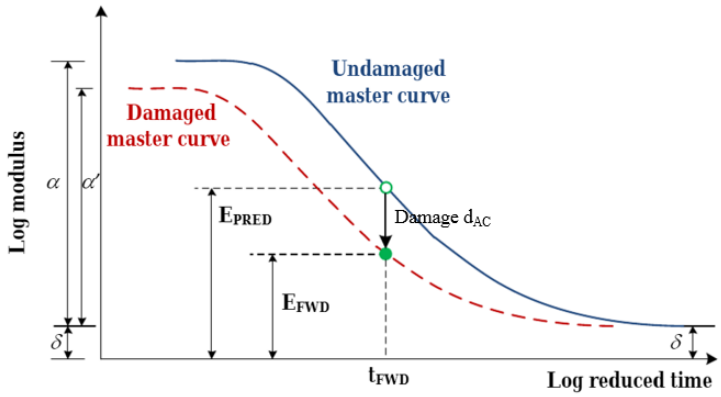

E_{PRED} = predicted modulus.

Figure 14. Illustration. Estimation of damage in AC layer using E_{FWD}.

When FWD measurements are not available, condition survey data can be used (option 2B-2B). Therefore, the amount of alligator cracking (i.e., bottom–up fatigue cracking) in the AC layer is used in the calibrated transfer function (figure 15) to determine d_{AC}.

$$FC_{AC} = \frac{100}{1 + e^{c_{f\text{-}bot} + d_{f\text{-}bot}(d_{AC})}}$$

Figure 15. Equation. Transfer function for calculating alligator cracking.

Where:

FC_{AC} = area of alligator cracking as a percent of total lane area.
$c_{f\text{-}bot}$ = field-calibrated fitting parameters for alligator cracking.
$d_{f\text{-}bot}$ = field-calibrated fitting parameters for damage in alligator cracking, which are defined by the equations in figure 16 and figure 17 (where H_{AC} is the thickness of the AC layer).[11]

$$c_{f\text{-}bot} = -2d_{f\text{-}bot}$$

Figure 16. Equation. First field-calibrated fitting parameter in the transfer function for calculating alligator cracking.

$$d_{f\text{-}bot} = -2.40874 + 39.748(1 + H_{AC})^{-2.856}$$

Figure 17. Equation. Second field-calibrated fitting parameter in the transfer function for calculating alligator cracking.

When neither FWD measurements nor condition surveys are available, the existing AC damage can be estimated using the general condition rating (option 2B-2C) given in table 5.[11] By knowing the damage and using the undamaged E^* master curve, the damaged E^* master curve can be obtained using the equation in figure 13.

Table 5. Recommended damage based on pavement-condition rating.

Pavement-Condition Rating	Description	Damage
Excellent	No cracking, minor rutting, and/or minor mixture-related distresses (e.g., raveling); little to no surface distortions or roughness.	0.0–0.2
Good	Limited load- and/or non-load-related cracking, moderate rutting, and/or moderate mixture-related distresses; some surface distortions or roughness.	0.2–0.4
Fair	Moderate load- and/or non-load-related cracking, moderate rutting, moderate amount of mixture-related distresses, and/or some roughness (IRI > 120 inches/mi).	0.4–0.8
Poor	Extensive non-load-related cracking, moderate load-related cracking, high rutting, extensive mixture-related distresses, and/or elevated levels of roughness (IRI > 170 inches/mi).	0.8–1.2
Very poor	Extensive load-related cracking, and/or very rough surfaces (IRI > 220 inches/mi).	>1.20

IRI = International Roughness Index.

CHAPTER 3. CHARACTERIZATION OF UNBOUND MATERIALS

M_R is an important material property for unbound materials (e.g., CAB and SG). The repeated triaxial M_R test is performed on the unbound materials over a wide range of confining stress (σ_c) and deviator stress (σ_d) to capture the stress dependency (i.e., nonlinearity) of unbound materials.[16] M_R is equal to the ratio of the applied σ_d to the recoverable strain (ε_r) when the applied load is retracted from the specimen (figure 18).

$$M_R = \frac{\sigma_d}{\varepsilon_r}$$

Figure 18. Equation. Calculation of M_R in repeated triaxial M_R test.

It is commonly accepted to treat an unbound layer as linear elastic in traditional pavement analysis procedures (e.g., standard-traffic loading). The FWD backcalculated unbound layer moduli are seen as appropriate since the stress conditions induced by FWD at common load levels (approximately 9,000 to 12,000 lb) and standard-traffic loading are considered similar. In the case of SHL vehicle–movement analysis, considering the same FWD backcalculated properties for the unbound layers may lead to improper estimation of pavement responses since different state-of-stress conditions are induced in the pavement layers. Hence, it is necessary to consider a stress-dependent M_R that reflects the stress state induced by the SHL vehicle on the unbound layers.

However, the M_R relationship as a function of stress state for unbound materials in a pavement analysis requires a finite element type of analysis, while the 3D-Move Analysis software assumes uniform properties that do not vary in the lateral direction. To overcome this limitation, an iterative approach incorporating the nonlinear, stress-dependent M_R relationship and the existing state of stresses in the unbound layers was employed in this project. This approach is described in this chapter.

3.1. DETERMINATION OF M_R RELATIONSHIP

Various relationships have been developed to represent the M_R relationship as a function of stress state. In this project, the Uzan model presented in figure 19 was adopted.[20] This model is capable of considering hardening and softening behaviors of unbound material by incorporating bulk stress (θ) and σ_d, respectively.

$$M_R = K\theta^n\sigma_d^m$$

Figure 19. Equation. Uzan model.

Where:

K = regression constant of resilient modulus model.
n = bulk stress exponent.
m = deviator stress exponent.

These regression constants can be obtained by conducting the repeated triaxial M_R test.[21] However, the time-consuming and destructive processes of sample collection and testing and the

associated costs are objectionable limitations. The stress dependency of unbound materials is usually reflected in E_{FWD} when multiple and distinct FWD load levels are applied.[22] Therefore, the use of FWD measurements at multiple load levels to estimate the regression constants of the stress-dependent M_R relationship was proposed. The set of E_{FWD} in conjunction with the corresponding load-induced state of stresses can be used to identify the regression constants. The following steps outline the approach:

1. The backcalculated-layer moduli values at each load level are used in the 3D-Move Analysis software to compute the stress tensor (σ_{ij}) at a representative element in the unbound layers when the applied load is simulated by uniform static loading. For the SG layer, an element located at the depth of 6 inches from the top of the SG and centerline of the load is treated as the representative element. For the other existing unbound layers in the pavement structure (e.g., the base and subbase), the representative element is selected at the middle of the layer.

2. The calculated induced σ_{ij} at the representative element is transformed into an equivalent laboratory triaxial stress testing condition by the use of stress invariants, similar to previous studies.[23,24] Stress invariant values are the same regardless of the orientation of the coordinate system chosen. The octahedral normal stress (σ_{oct}) and octahedral shear stress (τ_{oct}), which are invariants, are used to convert σ_{ij} computed in the representative element under the FWD loads to σ_d and σ_c in a triaxial test setup using the equations presented in figure 20 through figure 23. In these equations, σ_1, σ_2, and σ_3 are the major, intermediate, and minor principal stresses, respectively.

$$\sigma_{oct} = \frac{1}{3}(\sigma_1 + \sigma_2 + \sigma_3)$$

Figure 20. Equation. σ_{oct} calculation.

$$|\tau_{oct}| = \frac{1}{3}\sqrt{(\sigma_1 - \sigma_2)^2 + (\sigma_2 - \sigma_3)^2 + (\sigma_3 - \sigma_1)^2}$$

Figure 21. Equation. τ_{oct} calculation.

$$\sigma_d = \frac{3}{\sqrt{2}}|\tau_{oct}|$$

Figure 22. Equation. Triaxial simulated σ_d calculation.

$$\sigma_c = \sigma_{oct} - \frac{\sigma_d}{3}$$

Figure 23. Equation. Triaxial simulated σ_c calculation.

3. As presented in figure 24, the calculated σ_d and σ_c values at each load level can be used to compute the corresponding θ.

$$\theta = 3\sigma_c + \sigma_d$$

Figure 24. Equation. θ calculation.

4. By knowing E_{FWD} at each load level and the corresponding θ and σ_d, the regression constants for the Uzan model (figure 19) are then determined using the mean-square-error technique.

3.2. DETERMINATION OF REPRESENTATIVE M_R

As mentioned in section 1.1, the 3D-Move Analysis software is a finite layer method that assumes uniform linear elastic properties for the unbound pavement layers and the SG. In order to implement the nonlinear stress-dependent M_R of any unbound layer or SG, the M_R relationship for the layer that is discussed in section 3.1 must first be determined. By knowing the M_R relationship and state of stresses in the representative elements of the layer under consideration, the representative M_R value for the layer can be established. The following steps outline the approach:

1. Initial resilient moduli for the unbound layers are assumed (i.e., seed values). The material properties for the AC layer are identified using the approach described in chapter 2.

2. The nucleus of the SHL vehicle is determined using the 3D-Move Analysis software and seed moduli for the unbound layers. The methodology to determine the nucleus of an SHL vehicle can be found in Volume Ⅱ: Appendix B.[3]

3. Knowing the nucleus and material properties specified in step 1, σ_{ij} at a representative depth in the unbound layers within the domain specified by the length and width of the nucleus is computed. To be consistent with the determination of the M_R relationship (section 3.1), 6 inches from the top of the SG and the middle of the layers for the other existing unbound layers (e.g., base and subbase) are selected as the locations where σ_{ij} are computed.

4. The calculated induced σ_{ij} at the representative depth are employed to identify the σ_d, σ_c, and θ using the equations presented in figure 20 through figure 24.

5. From the calculated σ_d and θ, the M_R can be determined using the M_R relationship (figure 19).

6. The calculated M_R for each unbound layer is compared against the seed value chosen in step 1. If the difference between the two values is more than the threshold value (e.g., 5 percent), the calculated M_R from step 5 are used as seed values in step 2 with the 3D-Move Analysis software to calculate the new σ_{ij} at the locations specified in step 3.

7. Until the difference between the calculated M_R from two consecutive iterations is within 5 percent, step 2 through step 6 are repeated. The calculated M_R from the last iteration is considered as the representative M_R for the unbound layer under the evaluated SHL vehicle.

CHAPTER 4. OVERALL SUMMARY

Estimations of pavement responses under an SHL vehicle are required inputs for investigating the pavement structural adequacy. When determining the pavement responses using numerical models, such as the 3D-Move Analysis software, the first critical step is the material characterization of the existing pavement materials.

While pavement layers are traditionally assumed to be linear elastic, such an assumption in the case of SHL movements may result in an inappropriate estimation of pavement responses because of the difference in the characteristics of SHL vehicles compared to those of standard trucks (e.g., vehicle speed, axle and tire configurations, tire loading).

E^* is the primary material property of AC layers and is a function of temperature and loading frequency. The role of lower SHL-vehicle speeds in the pavement analysis can be addressed using the E^* master curve for the AC layer, which is a readily accepted input for the 3D-Move Analysis software. In order to incorporate existing damage into the existing AC layer, a methodology to estimate a field-damaged E^* master curve that considers the reduction in the AC-layer stiffness was proposed. The overall methodology that is consistent with the current approach used in the AASHTOWare® Pavement ME software is summarized in table 6.[13]

In the case of unbound materials, it is well accepted that the M_R of these materials is a function of stress state. It is believed that the induced state of stresses by FWD loading at the common load levels (approximately 9,000 to 12,000 lb) and a standard truck are similar. Therefore, E_{FWD} for unbound materials can be viewed as a representative stiffness in the pavement analysis when the standard truck traffic is of concern. However, in the case of SHL vehicles, higher states of stresses compared to those observed under a common FWD load level are expected. Consequently, the FWD-based E_{FWD} of an unbound layer may not represent the stiffness of the layer expected under SHL-vehicle movement. In order to overcome this issue and consider the stress dependency of unbound layers and the SG, an iterative approach incorporating a nonlinear, stress-dependent M_R relationship and the existing state of stresses in the unbound layers was employed in this project (table 7).

Table 6. Determination of field-damaged *E master curve for an AC layer.**

Main Steps	Options	Substeps	Suboptions	Required Inputs
Step 1. Determination of viscosity–temperature susceptibility relationship of asphalt binder.	Option 1A: Calculated *A* and *VTS* parameters from measured *G** and phase angle.	—	—	Recovered asphalt binder according to AASHTO T 319.(15) Measured asphalt binder *G** and phase angle at a minimum of three temperatures according to AASHTO T 315.(14)
Step 1. Determination of viscosity–temperature susceptibility relationship of asphalt binder.	Option 1B: Estimated *A* and *VTS* parameters from database.	—	—	Asphalt binder's PG or penetration grade.
Step 2. Construction of damaged *E** master curve.	Option 2A: Measured *E** on cores from wheel path.	—	—	Measured *E** according to AASHTO T 378 on core from wheel path.(16)
Step 2. Construction of damaged *E** master curve.	Option 2B: Estimated damaged *E** master curve.	Step 2B-1: Construction of undamaged *E** master curve.	Option 2B-1A: Measured *E** on cores from between wheel paths.	Measured *E** according to AASHTO T 378 on core from between the wheel paths.(16)
Step 2. Construction of damaged *E** master curve.	Option 2B: Estimated damaged *E** master curve.	Step 2B-1: Construction of undamaged *E** master curve.	Option 2B-1B: *E** predictive model (e.g., Witczak).	Asphalt-mixture volumetrics, V_a and V_{beff} (AASHTO T 166 and AASHTO T 209 or historical data).(17,18) Aggregate gradation (AASHTO T 319 and AASHTO T 30 or historical data).(15,19) Asphalt-binder η (AASHTO T 319 and AASHTO T 315 or historical data).(14,15)
Step 2. Construction of damaged *E** master curve.	Option 2B: Estimated damaged *E** master curve.	Step 2B-2: Damage characterization.	Option 2B-2A: Using backcalculated AC-layer modulus.	E_{FWD} of AC layer, *f*, and temperature at the middepth of AC layer.
Step 2. Construction of damaged *E** master curve.	Option 2B: Estimated damaged *E** master curve.	Step 2B-2: Damage characterization.	Option 2B-2B: Condition survey data.	Condition survey data (percent bottom–up fatigue cracking). Bottom–up fatigue cracking calibrated transfer function.
Step 2. Construction of damaged *E** master curve.	Option 2B: Estimated damaged *E** master curve.	Step 2B-2: Damage characterization.	Option 2B-2C: General condition rating.	Pavement-condition rating (excellent, good, fair, poor, and very poor).

—No data.

Table 7. Determination of representative M_R for an unbound layer.

Main Steps	Options	Substeps
Step 1. Determination of the M_R relationship.	Option 1A: Laboratory measured M_R according to AASHTO T 307.[21]	—
Step 1. Determination of the M_R relationship.	Option 1B: Using FWD data at multiple load levels.	Step 1B-1. Determine E_{FWD} at each load level. Step 1B-2. Compute σ_{ij} at the representative element of the layer. Step 1B-3. Calculate the equivalent triaxial σ_c, σ_d, and θ. Step 1B-4. Determine the regression constants for the M_R relationship.
Step 2. Determination of the representative M_R under an SHL vehicle.	—	Step 2-1. Assume the seed value for M_R of the unbound layer. Step 2-2. Determine the nucleus of the SHL vehicle. Step 2-3. Compute σ_{ij} at the representative element of the unbound layer. Step 2-4. Calculate the equivalent triaxial σ_c, σ_d, and θ. Step 2-5. Estimate M_R using the developed M_R relationship in step 1 in conjunction with calculated σ_d and θ. Step 2-6. Compare the estimated M_R with the seed value. If the difference is high (e.g., more than 5 percent), use the estimated value as a new seed value in step 2-2. Step 2-7. Repeat step 2-2 through step 2-7 until the differences between two consecutive iterations are less than 5 percent.

—No data.

REFERENCES

1. Hajj, E.Y., Siddharthan, R.V., Nabizadeh, H., Elfass, S, Nimeri, M., Kazemi, S.F., Batioja-Alvarez, D.D., and Piratheepan, M. (2018). *Analysis Procedures for Evaluating Superheavy Load Movement on Flexible Pavements, Volume I: Final Report*, Report No. FHWA-HRT-18-049, Federal Highway Administration, Washington, DC.

2. Nimeri, M., Nabizadeh, H., Hajj, E.Y., Siddharthan, R.V., Elfass, S, and Piratheepan, M. (2018). *Analysis Procedures for Evaluating Superheavy Load Movement on Flexible Pavements, Volume II: Appendix A, Experimental Program*, Report No. FHWA-HRT-18-050, Federal Highway Administration, Washington, DC.

3. Nimeri, M., Nabizadeh, H., Hajj, E.Y., Siddharthan, R.V., and Elfass, S. (2018). *Analysis Procedures for Evaluating Superheavy Load Movement on Flexible Pavements, Volume III: Appendix B, Superheavy Load Configurations and Nucleus of Analysis Vehicle*, Report No. FHWA-HRT-18-051, Federal Highway Administration, Washington, DC.

4. Nabizadeh, H., Hajj, E.Y., Siddharthan, R.V., Nimeri, M., Elfass, S., and Piratheepan, M. (2018). *Analysis Procedures for Evaluating Superheavy Load Movement on Flexible Pavements, Volume V: Appendix D, Estimation of Subgrade Shear Strength Parameters Using Falling Weigh Deflectometer*, FHWA-HRT-18-053, Federal Highway Administration, Washington, DC.

5. Nabizadeh, H., Nimeri, M., Hajj, E.Y., Siddharthan, R.V., Elfass, S., and Piratheepan, M. (2018). *Analysis Procedures for Evaluating Superheavy Load Movement on Flexible Pavements, Volume VI: Appendix E, Ultimate and Service Limit Analyses*, Report No. FHWA-HRT-18-054, Federal Highway Administration, Washington, DC.

6. Nabizadeh, H., Siddharthan, R.V., Elfass, S., and Hajj, E.Y. (2018). *Analysis Procedures for Evaluating Superheavy Load Movement on Flexible Pavements, Volume VII: Appendix F, Failure Analysis of Sloped Pavement Shoulders*, Report No. FHWA-HRT-18-055, Federal Highway Administration, Washington, DC.

7. Nabizadeh, H., Elfass, S., Hajj, E.Y., Siddharthan, R.V., Nimeri, M., and Piratheepan, M. (2018). *Analysis Procedures for Evaluating Superheavy Load Movement on Flexible Pavements, Volume VIII: Appendix G, Risk Analysis of Buried Utilities Under SHL Vehicle Moves*, Report No. FHWA-HRT-18-056, Federal Highway Administration, Washington, DC.

8. Batioja-Alvarez, D.D., Hajj, E.Y., and Siddharthan, R.V. (2018). *Analysis Procedures for Evaluating Superheavy Load Movement on Flexible Pavements, Volume IX: Appendix H, Analysis of Cost Allocation Associated with Pavement Damage Under a Superheavy Load Vehicle Move*, Report No. FHWA-HRT-18-057, Federal Highway Administration, Washington, DC.

9. Kazemi, S.F., Nabizadeh, H., Nimeri, M., Batioja-Alvarez, D.D., Hajj, E.Y., Siddharthan, R.V., and Hand, A.J.T. (2018). *Analysis Procedures for Evaluating Superheavy Load Movement on Flexible Pavements, Volume X: Appendix I, Analysis Package for Superheavy Load Vehicle Move on Flexible Pavement (SuperPACK)*, Report No. FHWA-HRT-18-058, Federal Highway Administration, Washington, DC.

10. 3D-Move Analysis software v2.1. (2013). Developed by University of Nevada, Reno, NV. Available online: http://www.arc.unr.edu/Software.html#3DMove, last accessed September 19, 2017.

11. National Cooperative Highway Research Program. (2004). *Guide for Mechanistic–Empirical Design of New and Rehabilitated Pavement Structures*, Final Report, Transportation Research Board, Washington, DC.

12. ASTM D2493/D2493M-16. (2016). "Standard Practice for Viscosity-Temperature Chart for Asphalt Binders." *Book of Standards, 04.03,* ASTM International, West Conshohocken, PA.

13. AASHTO. *AASHTOWare Pavement ME Design*, American Association of State Highway and Transportation Officials, Washington, DC. Available online: http://me-design.com/MEDesign/, last accessed July 2, 2018.

14. AASHTO T 315-12. (2016). *Standard Method of Test for Determining the Rheological Properties of Asphalt Binder Using a Dynamic Shear Rheometer (DSR)*, American Association of State Highway and Transportation Officials, Washington, DC.

15. AASHTO T 319. (2015). *Standard Method of Test for Quantitative Extraction and Recovery of Asphalt Binder From Asphalt Mixtures*, American Association of State Highway and Transportation Officials, Washington, DC.

16. AASHTO T 378-17. (2017). *Standard Method of Test for Determining the Dynamic Modulus and Flow Number for Asphalt Mixtures Using the Asphalt Mixture Performance Tester (AMPT)*, American Association of State Highway and Transportation Officials, Washington, DC.

17. AASHTO T 166-16. (2016). *Standard Method of Test for Bulk Specific Gravity (Gmb) of Compacted Hot Mix Asphalt (HMA) Using Saturated Surface-Dry Specimens*, American Association of State Highway and Transportation Officials, Washington, DC.

18. AASHTO T 209-12. (R2016). *Standard Method of Test for Theoretical Maximum Specific Gravity (Gmm) and Density of Hot-Mix Asphalt*, American Association of State Highway and Transportation Officials, Washington, DC.

19. AASHTO T 30-15. (2015). *Standard Method of Test for Mechanical Analysis of Extracted Aggregate*, American Association of State Highway and Transportation Officials, Washington, DC.

20. Uzan, J. (1985). "Characterization of Granular Materials." *Transportation Research Record, 1022*, pp. 52–59, Transportation Research Board, Washington, DC.

21. AASHTO T 307-99. (2017). *Standard Method of Test for Determining the Resilient Modulus of Soils and Aggregate Materials*, American Association of State Highway and Transportation Officials, Washington, DC.

22. Von Quintus, H.L. and Simpson, A.L. (2002). *Back-Calculation of Layer Parameters for LTPP Test Sections, Volume II: Layered Elastic Analysis for Flexible and Rigid Pavements*, Report No. FHWA-RD-01-113, Federal Highway Administration, Washington, DC.

23. Nabizadeh, H., Hajj, E.Y., Siddharthan, R., Elfass, S., and Nimeri, N. (2017). "Application of Falling Weight Deflectometer for the Estimation of In-Situ Shear Strength Parameters of Subgrade Layer." *Bearing Capacity of Roads, Railways, and Airfields*, pp. 743–749, Taylor & Francis Group, Milton Park, Didcot, United Kingdom.

24. Nabizadeh, H., Hajj, E.Y., Siddharthan, R., Elfass, S., and Sebaaly, P.E. (2016). "Estimation of In-Situ Shear Strength Parameters for Subgrade Layer Using Non-destructive Testing." *The Roles of Accelerated Pavement Testing in Pavement Sustainability*, pp. 525–538, Springer, Cham, Switzerland.

HRDI-20/10-18(WEB)E